

## Targeting Therapy with Mitosomal Daunorubicin plus Amlodipine Has the Potential To Circumvent Intrinsic Resistant Breast Cancer

Yan Zhang, Ruo-Jing Li, Xue Ying, Wei Tian, Hong-Juan Yao, Ying Men, Yang Yu, Liang Zhang, Rui-Jun Ju, Xiao-Xing Wang, Jia Zhou, Jing-Xian Chen, Nan Li, and Wan-Liang Lu\*

State Key Laboratory of Natural and Biomimetic Drugs and School of Pharmaceutical Sciences, Peking University, Beijing 100191, China

Received July 30, 2010; Revised Manuscript Received October 30, 2010; Accepted November 9, 2010

**Abstract:** Intrinsic resistance of cancers is a major cause of failure in chemotherapy. We proposed here a strategy to overcome intrinsic resistance by constructing cancer cell mitochondria-specifically targeting drug-loaded liposomes, namely, mitosomal daunorubicin plus amlodipine. Anticancer agent daunorubicin and apoptotic inducer amlodipine were loaded together into the mitosomes, and targeting molecule dequalinium was modified on the surface. Evaluations were performed on the breast cancer MCF-7 and resistant MCF-7/adr cells and in animals. Mitosomal daunorubicin plus amlodipine were about 97 nm, selectively accumulated in mitochondria, induced the swelling and disruption of mitochondria, dissipated the mitochondrial membrane potential, released a large amount of cytochrome C by translocation, cleaved Bid, and initiated a cascade of caspase 8 and 3 reactions. A robust anticancer effect was evidenced in vivo. Mitochondria-specifically targeting drug-loaded liposomes would provide a new strategy for treating resistant cancers.

**Keywords:** Intrinsic drug resistance; mitochondrial targeting; apoptosis; breast cancer; mitosomal daunorubicin plus amlodipine

### 1. Introduction

Chemotherapy plays a primary role in the management of cancers. However, the efficacy of chemotherapy seems to be discouraged due to the multidrug resistance (MDR) of cancers.<sup>1</sup> The primary mechanisms of MDR can be classified into two major types: acquired and intrinsic resistance. Acquired resistance could be derived from drug stimulus, leading to (a) the efflux of drug by the overexpression of cancer cell membrane protein ATP-binding cassette (ABC) transporters; (b) an increased drug-detoxifying function of cancer cells; and (c) the insensitivity of cancer cells to drug-

induced apoptosis.<sup>2</sup> The intrinsic resistance could come from (a) altered expression of apoptotic gene encoded proteins<sup>3</sup> or (b) genetic and epigenetic alterations in the activation of oncogenes and the inactivation of tumor suppression genes.<sup>4</sup> The intrinsic resistance of cancer has become the primary obstacle for chemotherapy.

In order to circumvent the drug resistance of cancers, we have developed two approaches. The first one was constructing antiresistant liposomes for targeting ABC transporters by incorporating anticancer agents together with MDR

\* Corresponding author. Mailing address: Peking University, School of Pharmaceutical Sciences, Xueyuan Road 38, Beijing 100191, China. Tel: +8610 8280 2683. Fax: +8610 8280 2683. E-mail: luwl@bjmu.edu.cn.

(1) Wu, H.; Hait, W. N.; Yang, J. M. Small interfering RNA-induced suppression of MDR1 (P-glycoprotein) restores sensitivity to multidrug-resistant cancer cells. *Cancer Res.* **2003**, *63*, 1515–9.

(2) Gottesman, M. M. Mechanisms of cancer drug resistance. *Annu. Rev. Med.* **2002**, *53*, 615–27.

(3) Johnstone, R. W.; Ruefli, A. A.; Lowe, S. W. Apoptosis: a link between cancer genetics and chemotherapy. *Cell* **2002**, *108*, 153–64.

(4) Kastrup, I. B.; Worm, J.; Ralfkiaer, E.; Hokland, P.; Guldberg, P.; Gronbaek, K. Genetic and epigenetic alterations of the reduced folate carrier in untreated diffuse large B-cell lymphoma. *Eur. J. Haematol.* **2008**, *80*, 61–6.

modulators.<sup>5</sup> The second was building specific liposomes for the cancer stem cells which lead to MDR and cancer metastasis, thereby killing the cancer cells and simultaneously eliminating the cancer stem cells.<sup>6</sup> As apoptosis plays a key role in chemotherapy,<sup>7</sup> we suggested a third strategy for suppressing intrinsic resistance by constructing cancer mitochondria-specifically targeting lipid nanovesicles named as mitosomes. Daunorubicin and amlodipine were incorporated together into the mitosomes, and dequalinium was modified on the mitosome surface as a targeting molecule.

Apoptosis is a process of programmed cell death involved in cellular stress response, and chemotherapy is to kill tumor cells mostly by apoptosis.<sup>8</sup> There are two major pathways for drug-induced apoptosis: one involves the cell surface receptors, while the other directly targets mitochondria.<sup>9</sup> Both of them seem to be focused on the mitochondrial level<sup>10,11</sup> because mitochondria play a major step-limiting role in the apoptosis of the cells.<sup>12</sup> Therefore, a number of experimental drugs have been used to act primarily on mitochondria to induce apoptosis of cancer cells, like betulinic acid.<sup>13</sup> However, the therapeutic effects are limited by little drug accumulation in mitochondria after administration.<sup>14</sup>

As a kind of polyethyleneglycol-containing lipid nanovesicles, the mitosomes are able to maintain the nature of pegylated liposomes which show enhanced permeability and retention (EPR) effects in tumor tissues and a reduction in

systemic side effects of anticancer agents.<sup>15</sup> Dequalinium is an amphiphilic cationic compound with a delocalized charge center which can accumulate in mitochondria of living cells in response to mitochondrial membrane potential.<sup>16</sup> It has been used for the delivery of DNA into mitochondria of living cells.<sup>17</sup> Daunorubicin is widely used in the treatment of a variety of malignancies.<sup>18</sup> It acts to kill cancers by inserting into DNA, interacting with DNA topoisomerase II, and producing reactive oxygen species.<sup>19</sup> Amlodipine is a dihydropyridine Ca<sup>2+</sup> channel blocker which has been proved to have capabilities in potentiating the apoptotic effect and in overcoming the resistance of cancers in our previous report.<sup>20</sup>

The objectives of the present study were to prepare the specific mitosomes, to evaluate their targeting therapy efficacy, and to define the mechanisms on human breast cancer MCF-7 and resistant MCF-7/adr cells in vitro and in animals.

## 2. Materials and Methods

### 2.1. Preparation and Characterization of Mitosomes.

Four types of nanovesicles were prepared, namely, daunorubicin plus amlodipine mitosomes which were used for mitochondria-specifically targeting therapy, daunorubicin liposomes, daunorubicin plus amlodipine liposomes, and blank mitosomes. The latter three were used as the controls.

- (5) Liang, G. W.; Lu, W. L.; Wu, J. W.; Zhao, J. H.; Hong, H. Y.; Long, C.; Li, T.; Zhang, Y. T.; Zhang, H.; Wang, J. C.; Zhang, X.; Zhang, Q. Enhanced therapeutic effects on the multi-drug resistant human leukemia cells in vitro and xenograft in mice using the stealthy liposomal vincristine plus quinacrine. *Fundam. Clin. Pharmacol.* **2008**, *22*, 429–37.
- (6) Liu, Y.; Lu, W. L.; Guo, J.; Du, J.; Li, T.; Wu, J. W.; Wang, G. L.; Wang, J. C.; Zhang, X.; Zhang, Q. A potential target associated with both cancer and cancer stem cells: a combination therapy for eradication of breast cancer using vinorelbine stealthy liposomes plus parthenolide stealthy liposomes. *J. Controlled Release* **2008**, *129*, 18–25.
- (7) Kroemer, G. de Th. H. Arsenic trioxide, a novel mitochondriotoxic anticancer agent? *J. Natl. Cancer Inst.* **1999**, *91*, 743–5.
- (8) Kroemer, G.; Dallaporta, B.; Resche-Rigon, M. The mitochondrial death/life regulator in apoptosis and necrosis. *Annu. Rev. Physiol.* **1998**, *60*, 619–42.
- (9) Green, D. R. Apoptotic pathways: the roads to ruin. *Cell* **1998**, *94*, 695–8.
- (10) Salvesen, G. S.; Dixit, V. M. Caspases: intracellular signaling by proteolysis. *Cell* **1997**, *91*, 443–6.
- (11) Soto-Cerrato, V.; Llagostera, E.; Montaner, B.; Scheffer, G. L.; Perez-Tomas, R. Mitochondria-mediated apoptosis operating irrespective of multidrug resistance in breast cancer cells by the anticancer agent prodigiosin. *Biochem. Pharmacol.* **2004**, *68*, 1345–52.
- (12) Green, D. R.; Reed, J. C. Mitochondria and apoptosis. *Science* **1998**, *281*, 1309–12.
- (13) Fulda, S.; Susin, S. A.; Kroemer, G.; Debatin, K. M. Molecular ordering of apoptosis induced by anticancer drugs in neuroblastoma cells. *Cancer Res.* **1998**, *58*, 4453–60.
- (14) D'Souza, G. G.; Weissig, V. Approaches to mitochondrial gene therapy. *Curr. Gene Ther.* **2004**, *4*, 317–28.
- (15) Lin, Y. Y.; Li, J. J.; Chang, C. H.; Lu, Y. C.; Hwang, J. J.; Tseng, Y. L.; Lin, W. J.; Ting, G.; Wang, H. E. Evaluation of pharmacokinetics of <sup>111</sup>In-labeled VNB-PEGylated liposomes after intraperitoneal and intravenous administration in a tumor/ascites mouse model. *Cancer Biother. Radiopharm.* **2009**, *24*, 453–60.
- (16) Modica-Napolitano, J. S.; Aprille, J. R. Delocalized lipophilic cations selectively target the mitochondria of carcinoma cells. *Adv. Drug Delivery Rev.* **2001**, *49*, 63–70.
- (17) Weissig, V.; Torchilin, V. P. Towards mitochondrial gene therapy: DQAsomes as a strategy. *J. Drug Targeting* **2001**, *9*, 1–13.
- (18) Simeonova, M.; Ivanova, G.; Enchev, V.; Markova, N.; Kamburov, M.; Petkov, C.; Devery, A.; O'Connor, R.; Brougham, D. Physicochemical characterization and in vitro behavior of daunorubicin-loaded poly(butylcyanoacrylate) nanoparticles. *Acta Biomater.* **2009**, *5*, 2109–21.
- (19) Oltersdorf, T.; Elmore, S. W.; Shoemaker, A. R.; Armstrong, R. C.; Augeri, D. J.; Belli, B. A.; Bruncko, M.; Deckwerth, T. L.; Dinges, J.; Hajduk, P. J.; Joseph, M. K.; Kitada, S.; Korsmeyer, S. J.; Kunzer, A. R.; Letai, A.; Li, C.; Mitten, M. J.; Nettesheim, D. G.; Ng, S.; Nimmer, P. M.; O'Connor, J. M.; Oleksijew, A.; Petros, A. M.; Reed, J. C.; Shen, W.; Tahir, S. K.; Thompson, C. B.; Tomaselli, K. J.; Wang, B. L.; Wendt, M. D.; Zhang, H. C.; Fesik, S. W.; Rosenberg, S. H. An inhibitor of Bcl-2 family proteins induces regression of solid tumours. *Nature* **2005**, *435*, 677–681.
- (20) Li, X.; Ruan, G. R.; Lu, W. L.; Hong, H. Y.; Liang, G. W.; Zhang, Y. T.; Liu, Y.; Long, C.; Ma, X.; Yuan, L.; Wang, J. C.; Zhang, X.; Zhang, Q. A novel stealth liposomal topotecan with amlodipine: apoptotic effect is associated with deletion of intracellular Ca<sup>2+</sup> by amlodipine thus leading to an enhanced antitumor activity in leukemia. *J. Controlled Release* **2006**, *112*, 186–98.

(1) *Blank Mitosomes*. Egg phosphatidylcholine (EPC), cholesterol, polyethylene glycol-distearoylphosphatidylethanolamine (PEG2000-DSPE, NOF Corporation, Japan) and dequalinium (Hangzhou Sanhe Chemicals, Co. Ltd., Hangzhou, China) (58/29/4/9,  $\mu\text{mol}$  ratio) were dissolved in chloroform and methanol (2:1, v/v) in a pear-shaped flask. The chloroform and methanol were evaporated to dryness under vacuum with a rotary evaporator, and then the formed lipid film was hydrated with 250 mM ammonium sulfate by sonication in the water bath for 10 min and followed by sonication using a probe-type sonicator for 7 min. The suspensions after hydration were successively extruded through polycarbonate membranes (Millipore, Bedford, MA, USA) with the pore size of 400 nm, and 200 nm 3 times, respectively. Then the blank mitosomes were obtained.

(2) *Daunorubicin plus Amlodipine Mitosomes*. The blank mitosomes were then dialyzed (12 000 to 14 000 molecular mass cutoff) in phosphate buffered saline (PBS, 137 mM NaCl, 2.7 mM KCl, 8 mM  $\text{Na}_2\text{HPO}_4$  and 2 mM  $\text{KH}_2\text{PO}_4$ , pH 7.4) 3 times (each time 12 h). Daunorubicin and amlodipine were loaded using an ammonium sulfate gradient loading method, as reported previously.<sup>21</sup> Appropriate amounts of daunorubicin hydrochloride (Nanjing Tianzun Zezhong Chemicals, Co. Ltd., Nanjing, China) and amlodipine besylate (Beijing Yimin Pharmaceuticals, Co. Ltd., Beijing, China) were added to the blank mitosomes. After mixing, the suspensions were incubated at 60 °C in a water bath, and intermittently shaken for 25 min to produce the daunorubicin plus amlodipine mitosomes.

(3) *Daunorubicin plus Amlodipine Liposomes*. The liposomes were prepared with the same procedures of daunorubicin plus amlodipine mitosomes, excluding the addition of dequalinium during film forming.

(4) *Daunorubicin Liposomes*. The liposomes were prepared with the same procedures of daunorubicin plus amlodipine liposomes, excluding the addition of amlodipine during drug loading.

Dequalinium, daunorubicin and amlodipine were determined with an ODS column (Dikma, 5  $\mu\text{m}$ , 250  $\times$  4.6 mm) by high performance liquid chromatography (HPLC) system with UV detector (Agilent Technologies Inc., Cotati, CA, USA). The mobile phase consisted of acetonitrile, 0.2 M  $\text{NaH}_2\text{PO}_4$ , methanol and triethylamine (34:66:2.4:0.3, v/v). The flow rate was set at 1.0 mL/min, and the detection wavelength was at 237 nm.

Dequalinium-modified nanovesicles were passed over a Sephadex G-50 column (Sigma-Aldrich Corporation, Beijing local agent, China) to remove the unmodified dequalinium. The modifying rate of dequalinium was calculated with the formula  $\text{MR} = (W_{\text{modifying}}/W_{\text{total}}) \times 100\%$ , where MR is the modifying rate of dequalinium,  $W_{\text{modifying}}$  is the measured amount of dequalinium in the liposome suspensions after

passing over the column, and  $W_{\text{total}}$  is the measured amount of dequalinium in the equal volume of nanovesicle suspensions before passing over the column. Similarly, the encapsulation efficiency of daunorubicin or amlodipine was measured through the same process and with a similar formula,  $\text{EE} = (W_{\text{encap}}/W_{\text{total}}) \times 100\%$ , where EE is the encapsulation efficiency of daunorubicin or amlodipine, and  $W_{\text{encap}}$  is the measured amount of daunorubicin or amlodipine in the nanovesicle suspensions after passing over the column.

The particle sizes, polydispersity indexes (PDI) and zeta potential values of all nanovesicles were measured with a Zetasizer 3000HSA (Malvern Instruments Ltd., U.K.).

To measure the in vitro release rates of daunorubicin and amlodipine encapsulated in the nanovesicles, a volume of 4 mL the nanovesicles was mixed with the release medium (1:1, v/v), sealed in dialysis tubing, and then immersed in 20.0 mL of the release medium, where the release medium was a mixture of phosphate buffered saline (PBS) and 10% fetal bovine serum (FBS). The dialysis was performed with an oscillator at a shaking rate of 100 times per minute at 37 °C. A volume of 0.5 mL of release medium was sampled at 0, 0.25, 0.5, 1, 2, 4, 6, 8, 12, 24, and 48 h, followed by immediate addition of an equal volume of fresh release medium, respectively. The content of daunorubicin or amlodipine was determined by HPLC as above. The release rate was estimated with the formula  $\text{RR} = (W_i/W_{\text{total}}) \times 100\%$ , where RR is the drug release rate (%),  $W_i$  is the measured drug amount of each sample, and  $W_{\text{total}}$  is the total drug amount in the equal volume of liposome suspensions before performing release experiment.

**2.2. Cell Culture.** Human breast cancer MCF-7 cells (obtained from Institute of Materia Medica, Chinese Academy of Medical Sciences and Peking Union Medical College, Beijing, China) and doxorubicin-resistant breast cancer MCF-7/adr cells (obtained from Institute of Hematology & Blood Diseases Hospital, Chinese Academy of Medical Sciences & Peking Union Medical College) were used. The culture medium was prepared with RPMI 1640 (Macgene Biotech Co., Ltd., Beijing, China) supplemented with 10% heat-inactivated fetal bovine serum (FBS, Macgene Biotech), 100 units/mL penicillin (Macgene Biotech), and 100 units/mL streptomycin (Macgene Biotech). The cell culture was performed in an incubator (37 °C and 5%  $\text{CO}_2$ ).

**2.3. Antiproliferative Activity.** MCF-7 or MCF-7/adr cells were seeded in a 96-well plate at a density of 9000 cells per well. After cells were cultured in an incubator for 24 h, fresh medium containing serial concentrations of various drug formulations was added into the plate well, including free daunorubicin (0–20  $\mu\text{M}$ ), free amlodipine (0–20  $\mu\text{M}$ ), free daunorubicin (0–20  $\mu\text{M}$ ) plus a fixed concentration of free amlodipine (2.5  $\mu\text{M}$ , 5  $\mu\text{M}$  or 10  $\mu\text{M}$ ), free daunorubicin (0–20  $\mu\text{M}$ ) plus free amlodipine (0–20  $\mu\text{M}$ ), blank mitosomes, liposomal daunorubicin plus amlodipine (both drugs in the range of 0–20  $\mu\text{M}$ ), and mitochondrial daunorubicin plus amlodipine (both drugs in the range of 0–20  $\mu\text{M}$ ). The mole ratio of daunorubicin to amlodipine was 1:1 when they were simultaneously incorporated into

(21) Ying, X.; Wen, H.; Lu, W. L.; Du, J.; Guo, J.; Tian, W.; Men, Y.; Zhang, Y.; Li, R. J.; Yang, T. Y.; Shang, D. W.; Lou, J. N.; Zhang, L. R.; Zhang, Q. Dual-targeting daunorubicin liposomes improve the therapeutic efficacy of brain glioma in animals. *J. Controlled Release* **2010**, *141*, 183–92.



one nanovesicle. After further incubation for 48 h, the antiproliferative activity was measured by sulforhodamine B (SRB) staining assay through reading the absorbance on a microplate reader (BIO-RAD model 680, Bio-Rad Laboratories, Inc. Shanghai, China) at the wavelength of 540 nm, as reported previously.<sup>21</sup> The survival rate was calculated with the following formula: survival % = ( $A_{540\text{nm}}$  for the treated cells/ $A_{540\text{nm}}$  for the control cells)  $\times$  100%, where  $A_{540\text{nm}}$  is the absorbance value. The dose–effect curves were plotted.

**2.4. Mitochondria-Targeting.** *2.4.1. Colocalization into the Mitochondria.* A confocal laser scanning fluorescent microscope with Leica confocal software (Leica, Heidelberg, Germany) was used to observe the mitochondria-targeting property of mitosomal daunorubicin plus amlodipine. Briefly, MCF-7 or MCF-7/adr cells were seeded into chambered coverslips at 170 000 cells per well. After incubation for 24 h, drugs were applied, respectively, including liposomal daunorubicin plus amlodipine (5  $\mu\text{M}$  for each drug), and mitosomal daunorubicin plus amlodipine (5  $\mu\text{M}$  for each drug, and 8.95  $\mu\text{M}$  for dequalinium). Following further incubation for 3 h, the cells were washed with PBS and then stained with Mitotracker Green FM (5  $\mu\text{M}$ , InvivoGen Corporation, Beijing local agent, China). Composite images were made by overlapping the images of the individual channels.

*2.4.2. Drug Content in the Mitochondrial Fraction.* Under the conditions of incubation (37 °C and 5%  $\text{CO}_2$ ), after applying liposomal daunorubicin plus amlodipine (20  $\mu\text{M}$  for each drug), mitosomal daunorubicin plus amlodipine (20  $\mu\text{M}$  for each drug) or blank medium for 3 h, MCF-7/adr cells were harvested. The isolation of mitochondria was performed according to the guide of cell mitochondria isolation kit (Beyotime Institute of Biotechnology, Haimen, China). Briefly, cells were reacted with mitochondria extraction reagent (provided in the kit) and stirred in a homogenizer. The suspensions were centrifuged at 600g for 10 min. The supernatants were collected and further centrifuged at 3500g for 10 min. The mitochondria were collected from the precipitates and stained with Mitotracker Green FM (5  $\mu\text{M}$ ) for 30 min. A confocal laser scanning fluorescent microscope was used to observe the drugs in the mitochondrial fraction, and a FAScan flow cytometer (Becton Dickinson FACS Calibur, Mountain View, CA, USA) was used to quantify the drug content in the mitochondrial fraction with the events collected 10 000.

**2.5. Structure of Mitochondria.** Mitochondria were isolated as above. After adding liposomal daunorubicin plus amlodipine (20  $\mu\text{M}$  for each drug), mitosomal daunorubicin plus amlodipine (20  $\mu\text{M}$  for each drug, 35.8  $\mu\text{M}$  for dequalinium), blank mitosomes (35.8  $\mu\text{M}$  for dequalinium), and blank medium, the suspensions were incubated for 30 min. The mitochondrial configurations were analyzed by transmission electron microscope (TEM, JEM-1400, JEOL Ltd., Tokyo, Japan).

**2.6. Mitochondrial Membrane Potential ( $\Delta\Psi_m$ ).** MCF-7 and MCF-7/adr cells were seeded in six-well plates at  $5 \times 10^5$  cells per well. After incubation for 24 h, the cells were

exposed to various formulations for 5 h, including free daunorubicin plus free amlodipine (10  $\mu\text{M}$  for each drug), liposomal daunorubicin (10  $\mu\text{M}$ ), liposomal daunorubicin plus amlodipine (10  $\mu\text{M}$  for each drug), mitosomal daunorubicin plus amlodipine (10  $\mu\text{M}$  for each drug), and fresh medium as control, respectively. Cells were harvested, washed with PBS 2 times, and stained with rhodamine-123 at 37 °C for 30 min. Considering rhodamine-123 is the substrate of the ABC proteins, the staining of MCF-7/adr was performed in the presence of MDR inhibitor verapamil hydrochloride (100  $\mu\text{M}$ ). Fluorescence intensity of rhodamine-123 accumulated in mitochondria was observed by FAScan flow cytometer.

**2.7. Release of Cytochrome C.** The translocation of cytochrome C from mitochondria to the cytosol was examined by immunohistochemical staining using streptavidin-peroxidase immunohistochemical kit (Zhongshan Goldenbridge Biotechnology, Co. Ltd., Beijing, China). Briefly, after incubation for 24 h, MCF-7 or MCF-7/adr cells were exposed to free amlodipine (10  $\mu\text{M}$ ), free daunorubicin (10  $\mu\text{M}$ ), free daunorubicin (10  $\mu\text{M}$ ) plus free amlodipine (10  $\mu\text{M}$ ), liposomal daunorubicin plus amlodipine (10  $\mu\text{M}$  for each drug) and mitosomal daunorubicin plus amlodipine (10  $\mu\text{M}$  for each drug), respectively. After incubation for another 24 h, cells were treated with 3%  $\text{H}_2\text{O}_2$ , blocking buffer (provided in the kit), primary antibody anticytochrome C (Nanjing KeyGen Biotechnology, Co., Ltd., Nanjing, China), enhanced secondary antibody (provided in the kit) and then enhanced streptavidin HRP conjugate (provided in the kit). After color development, release of cytochrome C was observed under a light microscope.

**2.8. Cleavage of Bid.** Bid is one of the proapoptotic Bcl-2 family proteins. The cleavage of Bid could enhance its proapoptotic activity.<sup>22</sup> The cleavage of Bid was measured using Bid ELISA kit (R&D Systems, Inc., Minneapolis, MN, USA; Shanghai local agent, China). Briefly, MCF/adr cells were cultured for 24 h, followed by addition of free daunorubicin (10  $\mu\text{M}$ ) plus free amlodipine (10  $\mu\text{M}$ ), liposomal daunorubicin (10  $\mu\text{M}$ ), liposomal daunorubicin plus amlodipine (10  $\mu\text{M}$  for each drug), and mitosomal daunorubicin plus amlodipine (10  $\mu\text{M}$  for each drug), respectively. The cells were further incubated for 12 h, collected and lysed. The cell lysates were centrifuged at 18000g at 4 °C for 12 min. Truncated Bid (tBid) was collected from the supernatants. Samples containing tBid were incubated in the wells of microplate processed by antibodies (provided in the kit) for 30 min. After being washed, the microplate was incubated with HRP-conjugate reagent (provided in the kit) for another 30 min. The substrates were added for color development light-tightly for 15 min. The cleavage of Bid was measured at 450 nm and the cleavage ratio was calculated according to the kit instructions.

(22) Chiang, P. C.; Chien, C. L.; Pan, S. L.; Chen, W. P.; Teng, C. M.; Shen, Y. C.; Guh, J. H. Induction of endoplasmic reticulum stress and apoptosis by a marine prostanoid in human hepatocellular carcinoma. *J Hepatol.* **2005**, *43*, 679–86.

### 2.9. Caspase 8 and 3 Activities by Luminescent Assays.

The activity of caspase 8 was measured using caspase 8 activity assay kit (Beyotime Institute of Biotechnology). Briefly, MCF-7/adr cells were cultured for 24 h. After addition of free daunorubicin (10  $\mu$ M) plus free amlodipine (10  $\mu$ M), liposomal daunorubicin (10  $\mu$ M), liposomal daunorubicin plus amlodipine (10  $\mu$ M for each drug), or mitosomal daunorubicin plus amlodipine (10  $\mu$ M for each drug), cells were incubated for another 12 h. The extraction procedure of caspase 8 was the same as that of Bid (as above). Caspase 8 substrate (provided in the kit) was changed into a yellow formazan product in the presence of caspase 8. Caspase 8 activity was measured at 405 nm on a microplate reader, and the activity ratio was calculated according to the kit instructions.

The procedures of measuring the activity of caspase 3 were the same as those for assaying caspase 8 but by using caspase 3 activity kit (Beyotime Institute of Biotechnology).

**2.10. In Vivo Inhibition of the Tumor Growth and TUNEL Analysis.** Female BALB/c nude mice, initially weighing 15–17 g, were obtained from Peking University Health Science Center. All animal experiments were performed in accordance with the principles of care and use of laboratory animals, and were approved by the Institutional Animal Care and Use Committee of Peking University. Briefly, approximately  $4 \times 10^6$  MCF-7/adr cells were resuspended in 200  $\mu$ L of serum-free medium, and injected subcutaneously into the right flanks of the nude mice. When tumors reached 100 to 150 mm<sup>3</sup> in volume, mice were randomly divided into five treatment groups (6 for each group). At day 23, 25, 28, 30, and 32 post inoculation, physiological saline, free daunorubicin (7.00 mg/kg) plus free amlodipine (7.04 mg/kg), liposomal daunorubicin (7.00 mg/kg), liposomal daunorubicin (7.00 mg/kg) plus amlodipine (7.04 mg/kg, mole ratio 1:1), and mitosomal daunorubicin (7.00 mg/kg) plus amlodipine (7.04 mg/kg, mole ratio 1:1) were given intravenously to mice which had been randomly divided into five treatment groups (6 for each) via tail vein, respectively. The mice were then monitored, and the inhibitory ratio of tumor volume was calculated with following formula: the inhibitory ratio for tumor volume (%) at day  $n = 100 \times V_n/V_{23}$ , where  $V_n$  represents the tumor volume at day  $n$ , and  $V_{23}$ , the tumor volume at day 23. Tumor volumes were calculated as length  $\times$  width<sup>2</sup>/2 (mm<sup>3</sup>).

At day 35, the mice were sacrificed. The tumors were excised and then fixed in paraformaldehyde (4%). Terminal deoxynucleotidyl transferase-mediated dUTP-biotin nick end labeling (TUNEL) assay was used to evaluate the apoptosis effect in the tumor tissue. The procedure was performed according to ApoapTag plus peroxidase in situ apoptosis detection kit (Intergen Co Ltd., Burlington, MA, USA) as reported previously.<sup>20,23</sup> Apoptotic cells manifested as brownish staining in the nuclei under the light microscope.

**2.11. Effects on the Hematological Indicators.** The preliminary safety evaluations were performed on female Kunming mice (initially weighing 15–17 g, Peking University Health Science Center). Twenty-five mice were

randomly divided into five groups (5 for each group). At day 3, 5, 8, 10, and 12, physiological saline, free daunorubicin (7.00 mg/kg) plus free amlodipine (7.04 mg/kg), liposomal daunorubicin (7.00 mg/kg), liposomal daunorubicin (7.00 mg/kg) plus amlodipine (7.04 mg/kg, mole ratio 1:1), and mitosomal daunorubicin (7.00 mg/kg) plus amlodipine (7.04 mg/kg, mole ratio 1:1) were given intravenously to mice via tail vein, respectively. The mice were sacrificed at day 15. Blood specimens of the mice were collected immediately. For each blood specimen, a portion of the whole blood was used for measuring the indicators of bone marrow in peripheral blood (white blood cells, WBC; hemoglobin, Hb; platelet, PLT). The rest of the blood was centrifuged at 3000 rpm for 10 min, and the serum was obtained for measuring liver function indicators (aspartate transaminase, AST; alanine transaminase ALT; total bilirubin, TB) and kidney function indicators (urea; creatinine, Cre).

**2.12. Statistics.** Data are presented as the mean  $\pm$  standard deviation. One-way analysis of variance was used to determine significance among groups, after which post hoc tests with the Bonferroni correction were used for comparison between individual groups. A value of  $P < 0.05$  was considered to be significant.

## 3. Results

**3.1. Characterization of Mitosomes.** In order to observe the effect of mitosomes, drug-loaded liposomes were also prepared and included for comparisons. For mitosomes prepared, the modifying rates of dequalinium were  $\geq 90\%$  (0.09  $\mu$ mol dequalinium/ $\mu$ mol lipids), and the encapsulation efficiencies of daunorubicin or amlodipine were  $\geq 95\%$ . For liposomes, the encapsulation efficiencies of daunorubicin or amlodipine reached the same level. For blank mitosomes, daunorubicin liposomes, daunorubicin plus amlodipine liposomes, and daunorubicin plus amlodipine mitosomes, the mean particle sizes were  $91.70 \pm 0.27$ ,  $100.93 \pm 0.42$ ,  $100.30 \pm 0.89$  and  $96.59 \pm 0.54$  nm, respectively. The potential values were  $-15.19 \pm 1.03$ ,  $-19.43 \pm 0.73$ ,  $-18.57 \pm 0.22$  and  $-13.28 \pm 0.89$  mV, respectively. For daunorubicin plus amlodipine mitosomes, the in vitro release rate of daunorubicin at 48 h was  $0.93 \pm 0.15\%$ , and that of amlodipine was  $4.56 \pm 0.34\%$ .

**3.2. Antiproliferative Activity.** Albeit daunorubicin alone resulted in obvious inhibitory effect in nonresistant MCF-7 cells, and free daunorubicin at various concentrations cotreated with a fixed concentration of free amlodipine exhibited a stronger inhibitory effect, respectively (Figure 1A<sub>1</sub>). When encapsulated into the nanovesicles, the inhibitory effect to

(23) Guo, J.; Zhou, J.; Ying, X.; Men, Y.; Li, R. J.; Zhang, Y.; Du, J.; Tian, W.; Yao, H. J.; Wang, X. X.; Ju, R. J.; Lu, W. L. Effects of stealth liposomal daunorubicin plus tamoxifen on the breast cancer and cancer stem cells. *J Pharm. Pharm. Sci.* **2010**, *13*, 136–51.

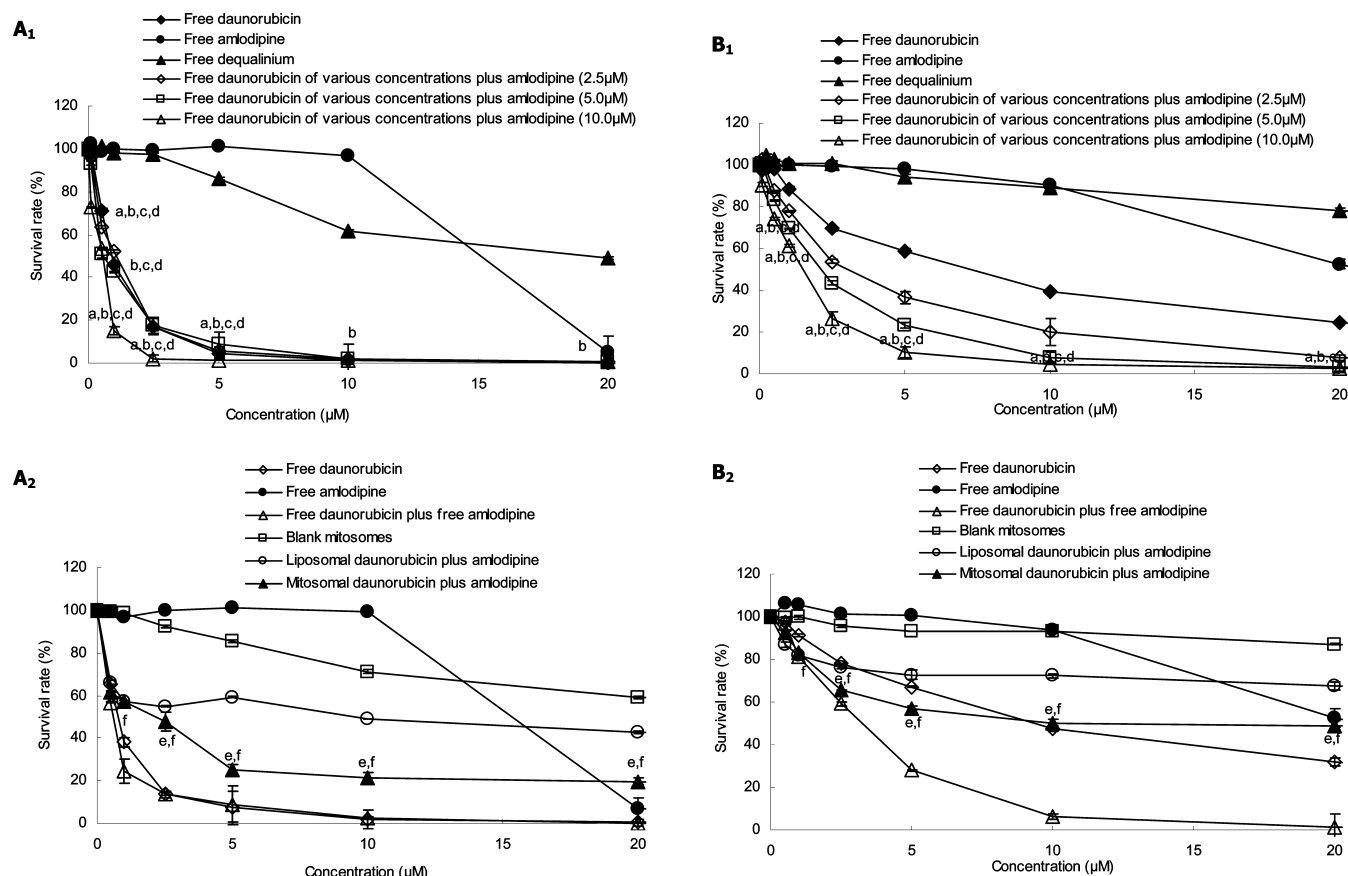


**Figure 1.** Effects of free daunorubicin, free amlodipine or free daunorubicin cotreated with free amlodipine, and various formulations on the proliferation of the MCF-7 (A<sub>1</sub>, A<sub>2</sub>), MCF-7/adr (B<sub>1</sub>, B<sub>2</sub>) measured by the sulforhodamine B (SRB) assay. Data are presented as the mean  $\pm$  SD ( $n = 3$ ). a,  $P < 0.05$ , versus free daunorubicin; b,  $P < 0.05$ , versus free amlodipine; c,  $P < 0.05$ , versus free daunorubicin of various concentrations plus amlodipine (2.5  $\mu$ M); d,  $P < 0.05$ , versus free daunorubicin of various concentrations plus amlodipine (5.0  $\mu$ M); e,  $P < 0.05$ , versus liposomal daunorubicin plus amlodipine; f,  $P < 0.05$ , versus blank mitosomes.

MCF-7 cells of mitosomal daunorubicin plus amlodipine was significantly higher than that of the liposomal daunorubicin plus amlodipine (Figure 1A<sub>2</sub>).

MCF-7/adr cells exhibited an evident resistance when applying free daunorubicin alone. In contrast, cytotoxicity of daunorubicin was increased markedly with the increase of amlodipine concentration, showing an amlodipine-dose dependent manner (Figure 1B<sub>1</sub>). When encapsulated into the nanovesicles, mitosomal daunorubicin plus amlodipine exhibited a stronger inhibitory effect to MCF-7/adr cells as compared to liposomal daunorubicin plus amlodipine (Figure 1B<sub>2</sub>).

**3.3. Mitochondria-Targeting.** **3.3.1. Colocalization into Mitochondria.** The confocal laser scanning microscopic images in Figures 2A and 2B represent the results after drugs were applied to MCF-7 cells, and the images in the Figures 2C and 2D denote those applied to MCF-7/adr cells, respectively. Mitochondria were seen as the green fluorescent color stained by Mitotracker (Figures 2A<sub>1</sub> and 2B<sub>1</sub>; Figures 2C<sub>1</sub>, and 2D<sub>1</sub>), and daunorubicin was shown as the red fluorescent color (Figures 2A<sub>2</sub> and 2B<sub>2</sub>; Figures 2C<sub>2</sub> and 2D<sub>2</sub>). The bright yellow fluorescence color (a composition of red and green fluorescence) demonstrated that daunorubicin was colocalized into mitochondria (Figures 2A<sub>3</sub> and 2B<sub>3</sub>; Figures 2C<sub>3</sub> and 2D<sub>3</sub>).

bicin was colocalized into mitochondria (Figures 2A<sub>3</sub> and 2B<sub>3</sub>; Figures 2C<sub>3</sub> and 2D<sub>3</sub>).

By judging from the yellow fluorescence, liposomal daunorubicin plus amlodipine were slightly colocalized into the mitochondria (Figures 2A<sub>1</sub> to 2A<sub>3</sub>; Figures 2C<sub>1</sub> to 2C<sub>3</sub>). On the contrary, mitosomal daunorubicin plus amlodipine were selectively accumulated into the mitochondria (Figures 2B<sub>1</sub> to 2B<sub>3</sub>; Figures 2D<sub>1</sub> to 2D<sub>3</sub>).

**3.3.2. Drug Content in the Mitochondrial Fraction.** Figures 3A and 3B represent the confocal laser scanning microscopic images in the isolated mitochondria after applying liposomal daunorubicin plus amlodipine or mitosomal daunorubicin plus amlodipine to MCF-7/adr cells for 3 h. Daunorubicin was shown as red fluorescent color (Figures 3A<sub>1</sub> and 3B<sub>1</sub>), and mitochondria were seen as green fluorescent color stained by Mitotracker (Figures 3A<sub>2</sub> and 3B<sub>2</sub>). The yellow fluorescence color was a composition of red and green fluorescence, and it indicated drug content in the mitochondrial fraction (Figures 3A<sub>3</sub> and 3B<sub>3</sub>). The bright red fluorescence in Figure 3B<sub>1</sub> and the bright yellow fluorescence in Figure 3B<sub>3</sub> showed that mitosomal daunorubicin plus amlodipine increased the drug content of



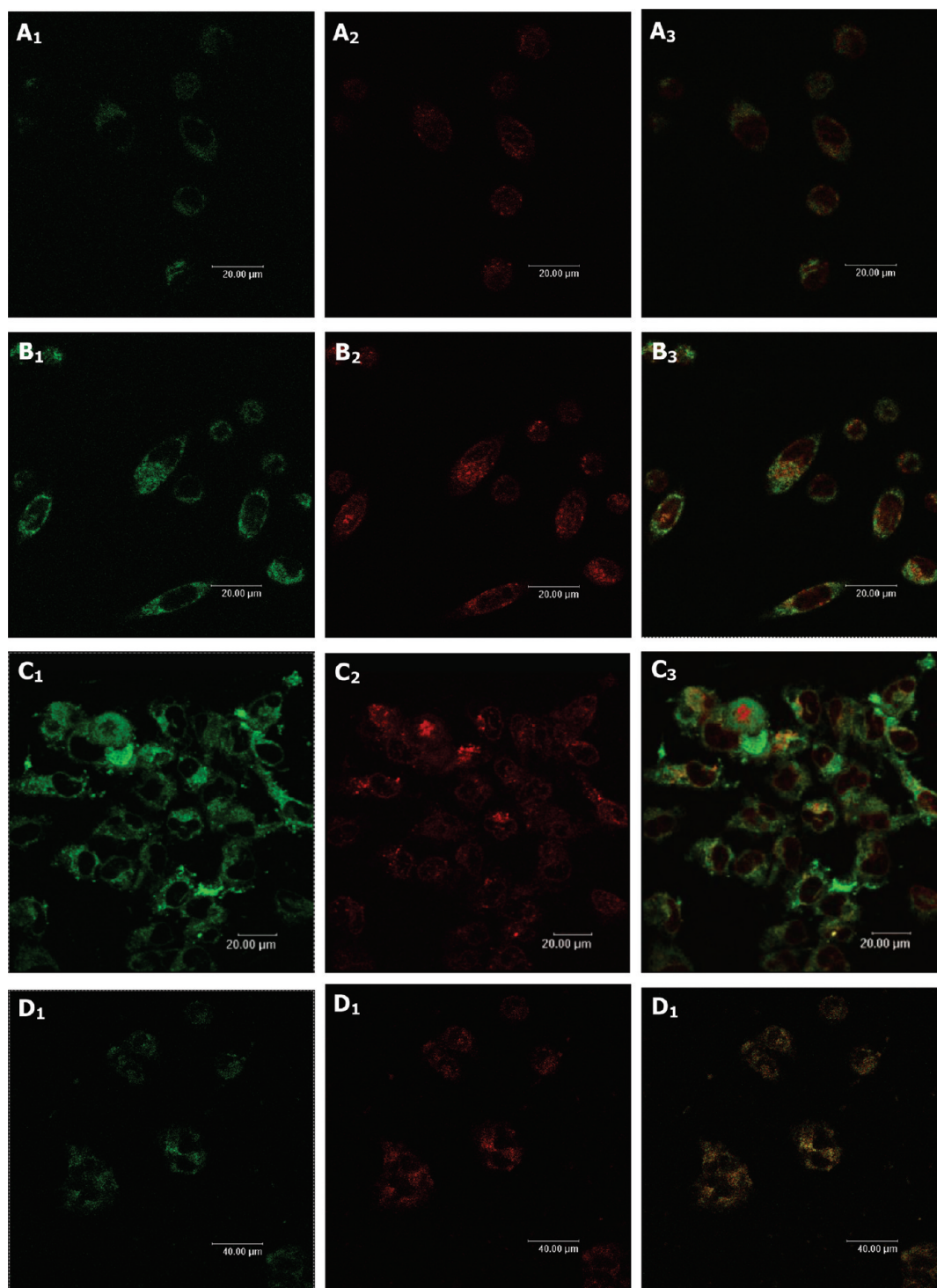


**Figure 2.** Colocalization of drugs into mitochondria by laser scanning microscopy (A to D). Live MCF-7 (A, B) and MCF-7/adr (C, D) cells were stained with Mitotracker Green and visualized after exposure to (A, C) liposomal daunorubicin plus amlodipine, (B, D) mitochondrial daunorubicin plus amlodipine. 1, green channel: Mitotracker Green stained mitochondria. 2, red channel: daunorubicin. 3, composite images of 1 and 2. The bright yellow fluorescence in B<sub>3</sub> or D<sub>3</sub> indicates that mitochondrial daunorubicin plus amlodipine are colocalized into the mitochondria.

mitochondrial fraction when compared to that in Figure 3A<sub>1</sub> or Figure 3A<sub>3</sub>.

Figure 3C shows the flow cytometric results in the isolated mitochondria after applying blank culture medium, liposomal daunorubicin plus amlodipine or mitochondrial daunorubicin plus

amlodipine to MCF-7/adr cells for 3 h. After applying mitochondrial daunorubicin plus amlodipine, the fluorescence intensity of the mitochondria was evidently higher than that after applying liposomal daunorubicin plus amlodipine. In quantitative evaluation for 10 000 events, the geometric mean intensity was 3.34 for blank

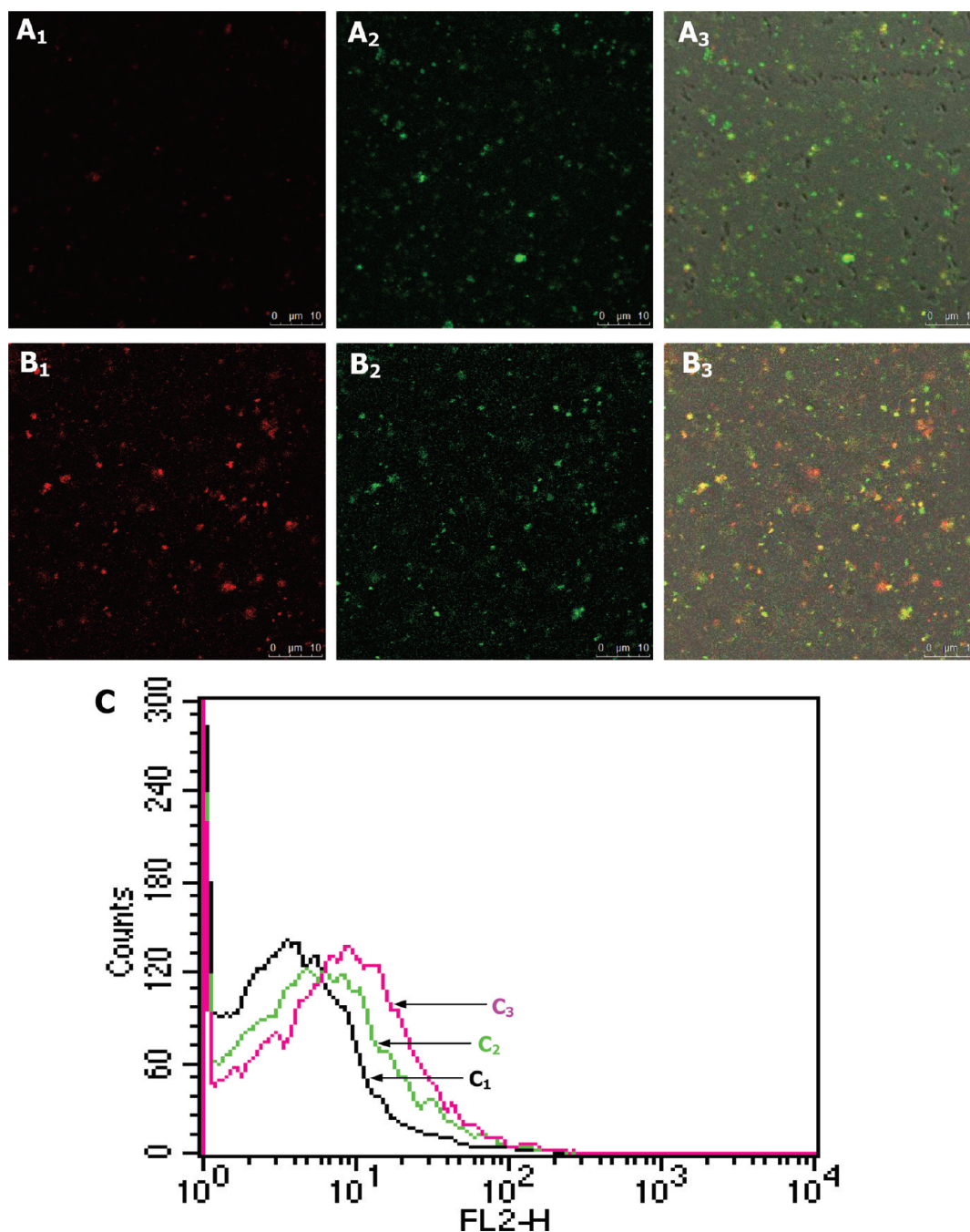


**Figure 3.** Drug content in mitochondrial fraction observed by laser scanning microscopy (A, B), and by FACScan flow cytometry (C). Mitochondria were isolated from MCF-7/adr cells after applying liposomal daunorubicin plus amlodipine (A), and mitosomal daunorubicin plus amlodipine (B) for 3 h incubation (37 °C and 5% CO<sub>2</sub>). A<sub>1</sub>, B<sub>1</sub>, green channel: mitochondria stained with Mitotracker green. A<sub>2</sub>, B<sub>2</sub>, red channel: daunorubicin. A<sub>3</sub>, B<sub>3</sub>, composite images of 1 and 2. The bright red fluorescence in B<sub>1</sub> and the bright yellow fluorescence in B<sub>3</sub> indicate that the treatment of mitosomal daunorubicin plus amlodipine increases the drug content in the mitochondrial fraction. In the flow cytometric experiment, results further demonstrate that the treatment of mitosomal daunorubicin plus amlodipine increases the drug content in the mitochondrial fraction of MCF-7/adr cells (C). C<sub>1</sub>, blank medium; C<sub>2</sub>, liposomal daunorubicin plus amlodipine; C<sub>3</sub>, mitosomal daunorubicin plus amlodipine.

control (Figure 3C<sub>1</sub>), 5.11 for liposomal daunorubicin plus amlodipine (Figure 3C<sub>2</sub>), and 6.60 for mitosomal daunorubicin plus amlodipine (Figure 3C<sub>3</sub>).

**3.4. Structure of Mitochondria.** Mitochondrion plays a critical role in the energy conversion which requests a strict microenvironment. Therefore the inner mitochondrial mem-

brane is impermeable even to tiny solutes and ions.<sup>24</sup> Results from TEM observations showed that the mitochondria of nontreated cells had a configuration with clear cristae, and complete inner/outer membranes (Figure 4A). In contrast, the treatment with mitosomal daunorubicin plus amlodipine caused disruption of the inner mitochondrial membrane and



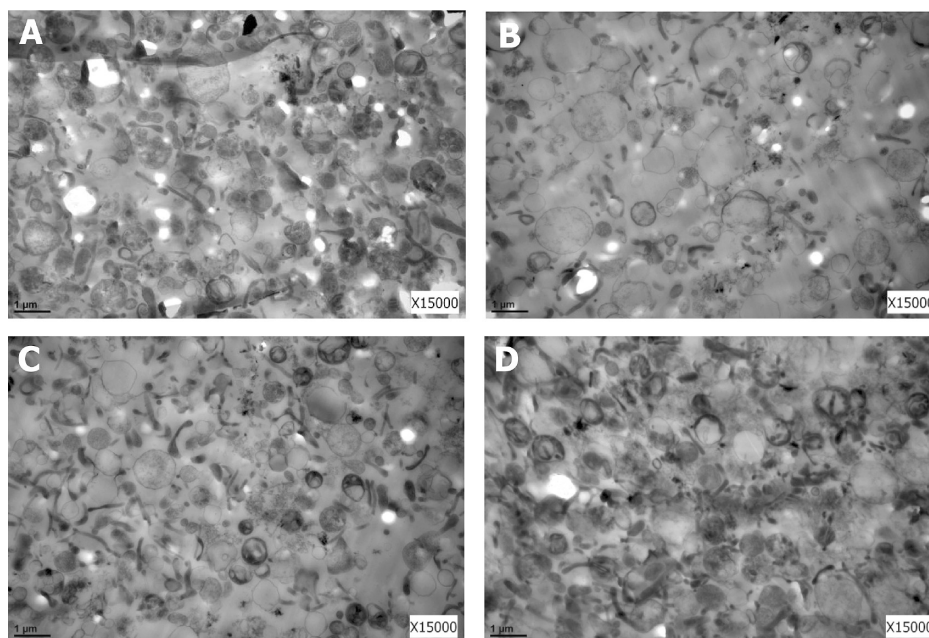


**Figure 4.** Transmission electron micrographs of the isolated mitochondria of MCF-7/adr cells treated with (A) blank culture medium as the control, (B) mitochondria-specific drug-loaded liposomes, (C) blank liposomes, and (D) free liposomes, respectively. The images were captured by the transmission electron microscope (TEM). The mitochondria treated with blank culture medium exhibit clear cristae and complete inner/outer membranes (A) while the mitochondria treated with the mitochondria-specifically targeting drug-loaded liposomes show an evident swelling of mitochondrial matrix and a disruption of inner mitochondrial membrane (B). In contrast, the mitochondria treated with blank liposomes display a slight swelling of mitochondrial matrix (C), and free liposomes does not affect the mitochondrial configuration (D).

swelling of the mitochondrial matrix (Figure 4B). As the controls, treatment with blank liposomes (containing dequalinium alone) caused a slight change of the mitochondrial configuration (Figure 4C), and treatment with free liposomes did not affect the mitochondrial configuration (Figure 4D).

**3.5. Mitochondrial Membrane Potential ( $\Delta\Psi_m$ ).** The  $\Delta\Psi_m$  was estimated by the fluorescence intensity of rhodamine-123 accumulated in the mitochondria. Rhodamine-123 is a fluorescent dye which could be incorporated into mitochondria and retained proportionally to the transmembrane potential, thus being used to measure the  $\Delta\Psi_m$ .<sup>25,26</sup> Data from flow cytometry showed that the exposure of mitochondria-specific drug-loaded liposomes resulted in an evident loss of the mitochondrial membrane potential of

MCF-7 (Figure 5A) and MCF-7/adr (Figure 5B) cells, as compared to free liposomes plus amlodipine or other controls.

**3.6. The Release of Cytochrome C.** Images in Figure 6A<sub>1</sub>–F<sub>1</sub> represent the data of MCF-7 cells, and those in Figure 6A<sub>2</sub>–F<sub>2</sub> depict the data of MCF-7/adr cells. Results showed that mitochondria-specific drug-loaded liposomes induced a large amount of cytochrome C releasing from mitochondria (Figure 6E<sub>1</sub>; Figure 6E<sub>2</sub>), evidenced by brown staining. In contrast, the images in control groups exhibited fewer brown regions in the cytosol when cells were exposed to free amlodipine (Figure 6B<sub>1</sub>; Figure 6B<sub>2</sub>), free daunorubicin (Figure 6C<sub>1</sub>; Figure 6C<sub>2</sub>), free liposomes plus amlodipine (Figure 6D<sub>1</sub>; Figure 6D<sub>2</sub>) or free daunorubicin plus free amlodipine (Figure 6F<sub>1</sub>; Figure 6F<sub>2</sub>).

**3.7. Cleavage of Bid.** Assay with the resistant MCF/adr cells showed that the cleavage of Bid was markedly increased by applying various formulations, as compared to that by applying the blank control (Figure 7A). In comparisons, the cleavage of pro-apoptotic protein Bid in the cells was the most eminently evidenced by applying mitochondria-specific drug-loaded liposomes plus amlodipine.

**3.8. Caspase 8 and 3 Activities.** When MCF-7/adr cells were exposed to various drugs, all treatment groups showed evident activities of caspase 8 (Figure 7B). The rank of caspase 8 activity was mitochondria-specific drug-loaded liposomes plus amlodipine > free daunorubicin plus free amlodipine ≥ free liposomes

- (24) Shinohara, Y.; Almofti, M. R.; Yamamoto, T.; Ishida, T.; Kita, F.; Kanzaki, H.; Ohnishi, M.; Yamashita, K.; Shimizu, S.; Terada, H. Permeability transition-independent release of mitochondrial cytochrome c induced by valinomycin. *Eur. J. Biochem.* **2002**, *269*, 5224–30.
- (25) Sancho, P.; Galeano, E.; Nieto, E.; Delgado, M. D.; Garcia-Perez, A. I. Dequalinium induces cell death in human leukemia cells by early mitochondrial alterations which enhance ROS production. *Leuk. Res.* **2007**, *31*, 969–78.
- (26) Finucane, D. M.; Waterhouse, N. J.; Amarante-Mendes, G. P.; Cotter, T. G.; Green, D. R. Collapse of the inner mitochondrial transmembrane potential is not required for apoptosis of HL60 cells. *Exp. Cell Res.* **1999**, *251*, 166–74.

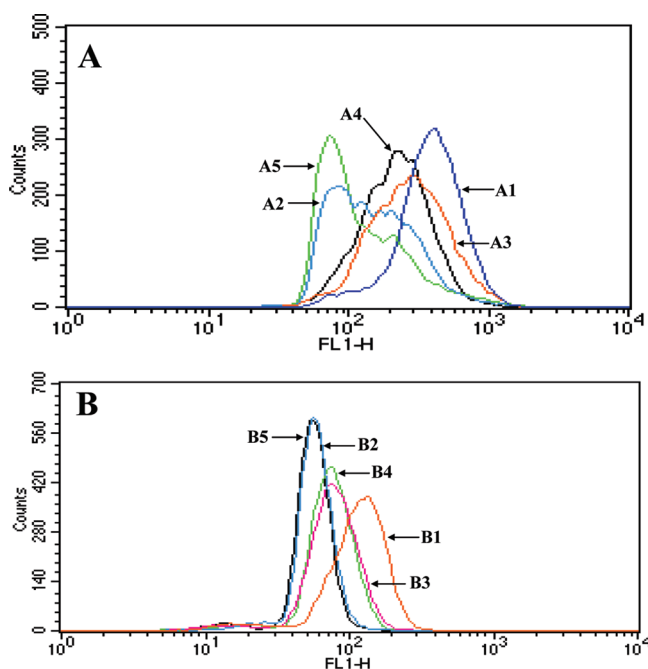


**Figure 5.** Dissipation of mitochondria membrane potential ( $\Delta\Psi_m$ ) measured by flow cytometry. Live MCF-7 (A) and MCF-7/adr cells (B) were stained with rhodamine-123 after exposure to various formulations, including blank control (A1, B1), free daunorubicin plus free amlodipine (A2, B2), liposomal daunorubicin (A3, B3), liposomal daunorubicin plus amlodipine (A4, B4), and mitosomal daunorubicin plus amlodipine (A5, B5) for 5 h. As compared to the liposomes unmodified with dequalinium, or the other controls, the exposure of mitosomal daunorubicin plus amlodipine leads to an obvious dissipation in the  $\Delta\Psi_m$ .

daunorubicin plus amlodipine > liposomal daunorubicin > the blank control. Results from caspase 3 assay showed a similar trend as that of caspase 8, as shown in Figure 7C.

### 3.9. Tumor Growth Inhibition and TUNEL Analysis.

After inoculation of MCF-7/adr cells in nude mice, the tumors reached suitable masses for treatment at day 23. As compared to blank control group, the inhibitory effects of tumor growth were obviously observed in all treatment groups. The rank of inhibitory effects was mitosomal daunorubicin plus amlodipine > liposomal daunorubicin plus amlodipine > free daunorubicin plus free amlodipine > liposomal daunorubicin > the blank control (Figure 8).

The TUNEL assay showed that the apoptotic percentages were  $1.83 \pm 0.29\%$  for the group treated with physiological saline (Figure 9A),  $5.17 \pm 0.76\%$  for the group treated with liposomal daunorubicin (Figure 9B),  $5.67 \pm 1.04\%$  for the group treated with free daunorubicin plus free amlodipine (Figure 9C),  $11.17 \pm 1.26\%$  for the group treated with liposomal daunorubicin plus amlodipine (Figure 9D), and  $17.83 \pm 2.02\%$  for the group treated with mitosomal daunorubicin plus amlodipine (Figure 9E).

**3.10. Effects on the Hematological Indicators.** Table 1 shows the effects of various formulations on the hemato-

logical indicators of bone marrow, liver function and renal function. After administration of mitosomal daunorubicin plus amlodipine, the levels of ALT, AST, TB, urea, and Cre in serum were slightly elevated, and those of WBC, Hb, and PLT in whole blood were slightly decreased, but without significant difference as compared to those after giving blank control.

After administration of liposomal daunorubicin or liposomal daunorubicin plus amlodipine, the levels of these indicators were similarly affected. Among these indicators, the level of WBC was severely lowered.

In contrast, after administration of free daunorubicin plus amlodipine, the level of ALT was significantly increased while those of WBC and PLT were evidently decreased. Nevertheless, the levels of AST, TB, urea, and Cre were slightly affected.

## 4. Discussion

Mitochondria are membrane-enclosed organelles (0.5–10  $\mu\text{m}$ ) acting as “cellular power plants” by generating most of the cell’s supply of adenosine triphosphate (ATP). Mitochondria are also involved in a range of other processes, such as signaling, cellular differentiation, and cell death, as well as the control of the cell cycle and cell growth.<sup>27</sup> Cancer mitochondria are concerned because the intrinsic drug resistance of cancers is closely associated with mitochondria which play a key role in apoptosis with all the apoptotic pathways converging on them.<sup>7,8</sup> The mitosomes could induce apoptosis by direct and indirect targeting mitochondria which initiate a cascade of pro-apoptotic reactions.

Many compounds have been developed for reversing MDR such as PSC833<sup>28</sup> and lanquidar (R101933).<sup>29</sup> However, when administered as the unencapsulated forms like solution injections, the drugs cannot be delivered to the tumor sites simultaneously due to different pharmacokinetics of an anticancer agent and a reversing agent, thus affecting the reversal efficacy of resistance. Incorporating anticancer agent and MDR modulator in the same vesicle would be beneficial for pharmacokinetic distribution of the drugs. The drug-loaded mitosomes could be delivered to and restrained in tumor tissue simultaneously by the EPR effect<sup>30</sup> and decrease the systemic side effects due to indirect exposure.

(27) McBride, H. M.; Neuspiel, M.; Wasiak, S. Mitochondria: more than just a powerhouse. *Curr. Biol.* **2006**, *16*, R551–60.

(28) Desrayaud, S.; Guntz, P.; Scherrmann, J. M.; Lemaire, M. Effect of the P-glycoprotein inhibitor, SDZ PSC 833, on the blood and brain pharmacokinetics of colchicine. *Life Sci.* **1997**, *61*, 153–63.

(29) Luurtsema, G.; Schuit, R. C.; Klok, R. P.; Verbeek, J.; Leysen, J. E.; Lammertsma, A. A.; Windhorst, A. D. Evaluation of [<sup>111</sup>C]laniquidar as a tracer of P-glycoprotein: radiosynthesis and biodistribution in rats. *Nucl. Med. Biol.* **2009**, *36*, 643–9.

(30) Kale, A. A.; Torchilin, V. P. Environment-responsive multifunctional liposomes. *Methods Mol. Biol.* **2010**, *605*, 213–42.



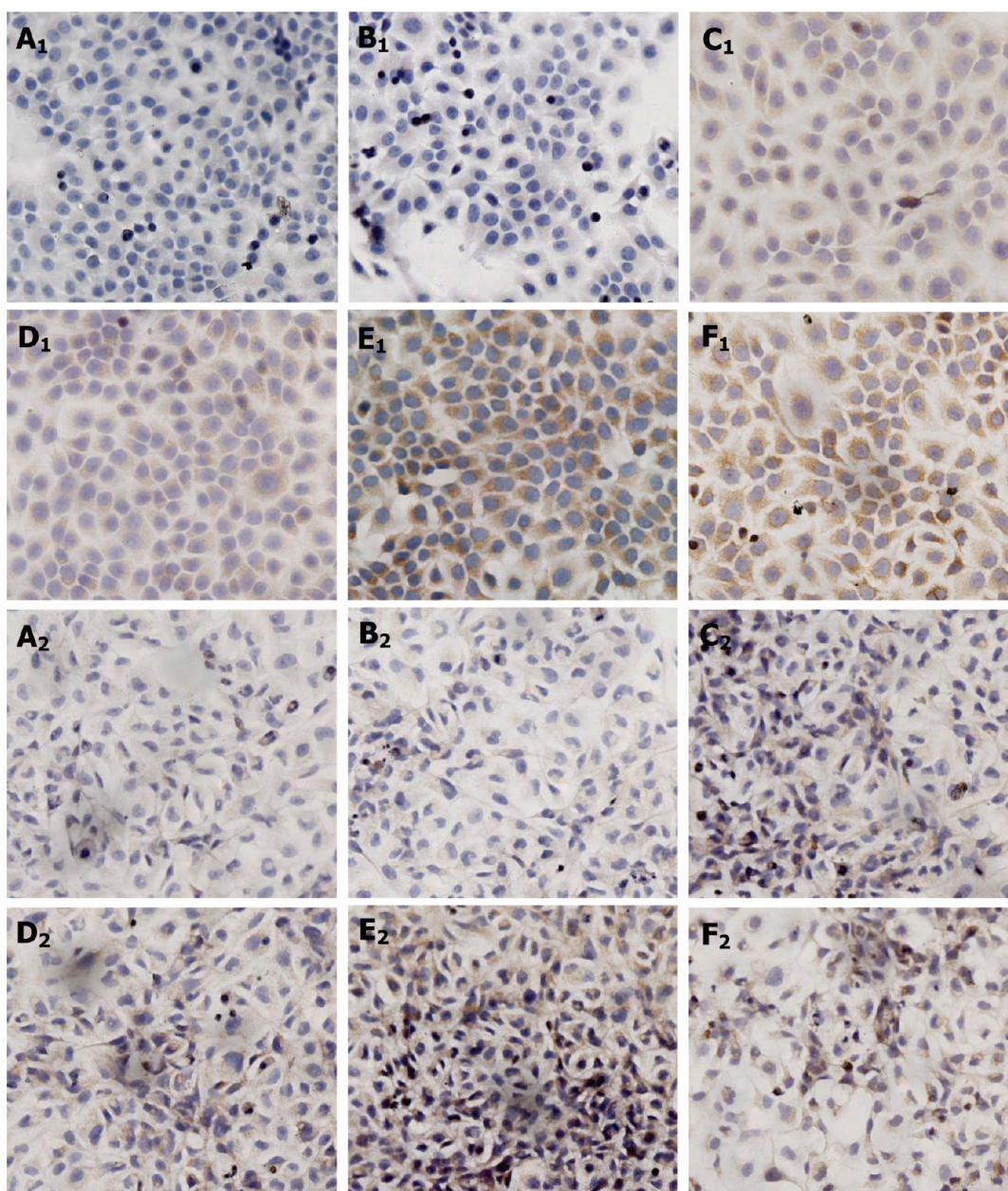


**Figure 6.** Immunohistochemical staining results of cytochrome C translocated from mitochondria to cytosol in the MCF-7 (subscripted by 1) and MCF-7/adr (subscripted by 2) cells by applying various formulations, including blank control (A<sub>1</sub>, A<sub>2</sub>), free amlodipine (B<sub>1</sub>, B<sub>2</sub>), free daunorubicin (C<sub>1</sub>, C<sub>2</sub>), liposomal daunorubicin plus amlodipine (D<sub>1</sub>, D<sub>2</sub>), mitosomal daunorubicin plus amlodipine (E<sub>1</sub>, E<sub>2</sub>), and free daunorubicin plus free amlodipine (F<sub>1</sub>, F<sub>2</sub>), respectively. The broad brown regions in the pictures E<sub>1</sub> and E<sub>2</sub> demonstrate the large amount release of cytochrome C.

Dequalinium is an amphiphilic cation showing an intrinsic mitochondriotropism.<sup>31</sup> A kind of vesicle made by dequalinium alone has been previously used for delivering DNA to mitochondria.<sup>32</sup> In the present study, dequalinium is modified on the surface

of the mitosomes aiming at the same intention for targeting mitochondria. The confocal laser scanning microscopic images indicate that the modifying of dequalinium on the drug-loaded nanovesicles is able to achieve an evident mitochondria-targeting property. The bright yellow fluorescence in the whole cells (Figures 2B<sub>3</sub> and 2D<sub>3</sub>) or in the isolated mitochondria (Figure 3B<sub>3</sub>) provides direct evidence for the colocalization of dequalinium-modified mitosomes into the mitochondria. In a semiquantitative way, flow cytometric measurement gives the relative drug content in the mitochondrial fraction, showing that the administration of mitosomal daunorubicin plus amlodipine increases the drug content in the mitochondrial fraction of MCF-7/adr cells (Figure 3C).

- (31) Weiss, M. J.; Wong, J. R.; Ha, C. S.; Bleday, R.; Salem, R. R.; Steele, G. D., Jr.; Chen, L. B. Dequalinium, a topical antimicrobial agent, displays anticarcinoma activity based on selective mitochondrial accumulation. *Proc. Natl. Acad. Sci. U.S.A.* **1987**, *84*, 5444–8.
- (32) D'Souza, G. G.; Rammohan, R.; Cheng, S. M.; Torchilin, V. P.; Weissig, V. DQAsome-mediated delivery of plasmid DNA toward mitochondria in living cells. *J. Controlled Release* **2003**, *92*, 189–97.



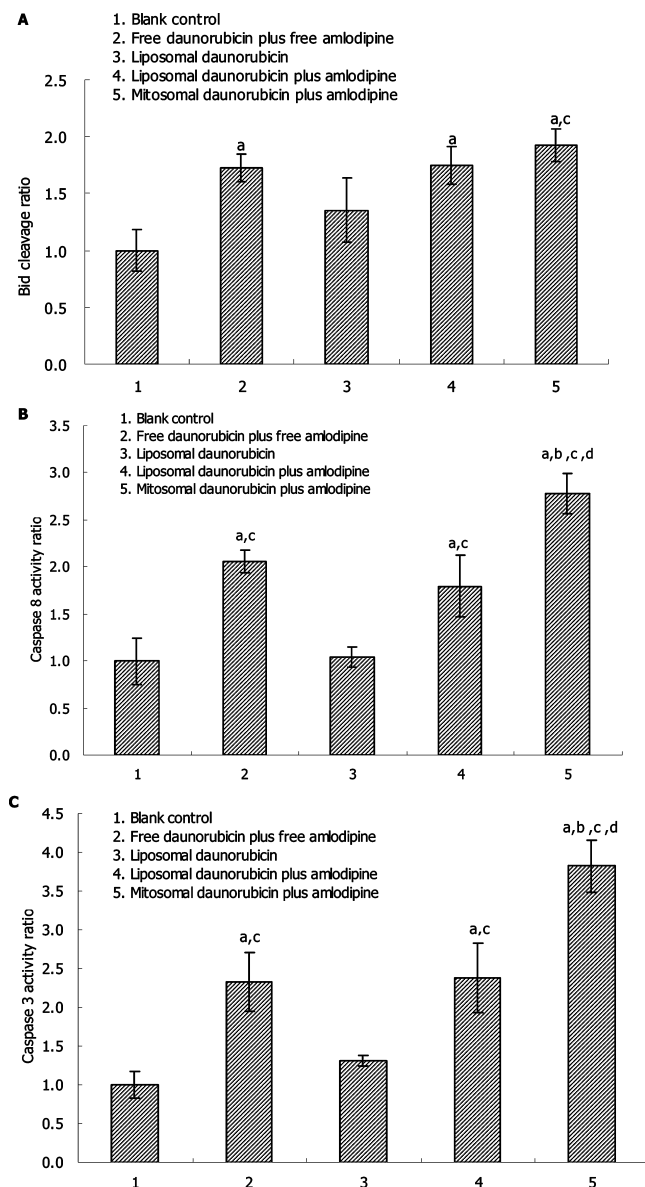


**Figure 7.** Cleavage of Bid (A) and activation of caspase 8 (B) and caspase 3 (C) in MCF-7/adr cells induced by various formulations. Data are presented as the mean  $\pm$  SD ( $n = 3$ ). Bid is a pro-apoptotic protein belonging to Bcl-2 family which plays an important role in the apoptosis. Mitosomal daunorubicin plus amlodipine induce the strongest effect on the activation of Bid and caspase 8 and 3. a,  $P < 0.05$ , versus blank control; b,  $P < 0.05$ , versus free daunorubicin plus free amlodipine; c,  $P < 0.05$ , versus liposomal daunorubicin; d,  $P < 0.05$ , versus liposomal daunorubicin plus amlodipine.

The mitochondria targeting of mitosomes is further evidenced by the change of mitochondrial structure under TEM and the decrease of  $\Delta\Psi_m$  analyzed by flow cytometry, and the release of cytochrome C in the immunohistochemical staining assay, as discussed below.

In the TEM images of the isolated mitochondria, phenomena like the disruption of the inner mitochondrial membrane and the swelling of mitochondrial matrix are consistent with those of mitochondria after being triggered

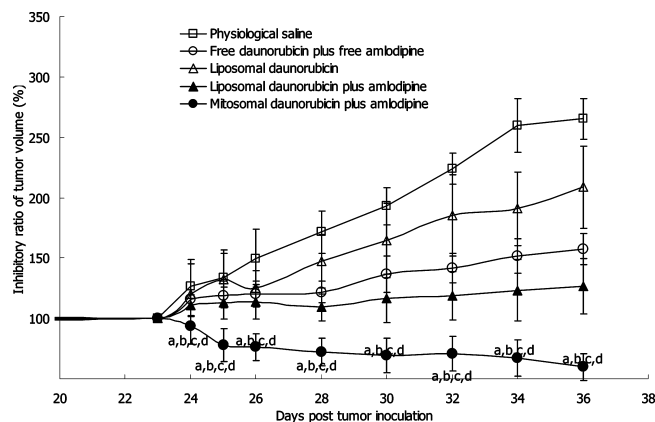


**Figure 8.** Effect of mitosomal daunorubicin plus amlodipine on the MCF-7/adr xenografts in female nude mice. At day 23, 25, 28, 30 and 32 after inoculation, physiological saline, free daunorubicin (7 mg/kg) plus free amlodipine (7.04 mg/kg, mole ratio 1:1), liposomal daunorubicin (7 mg/kg), liposomal daunorubicin (7 mg/kg) plus amlodipine (7.04 mg/kg, mole ratio 1:1), and mitosomal daunorubicin (7 mg/kg) plus amlodipine (7.04 mg/kg, mole ratio 1:1) were given intravenously to mice via tail vein, respectively. Data are presented as the mean  $\pm$  SD ( $n = 6$ ). a,  $P < 0.05$ , versus physiological saline; b,  $P < 0.05$ , versus free daunorubicin plus free amlodipine; c,  $P < 0.05$ , versus liposomal daunorubicin; d,  $P < 0.05$ , versus liposomal daunorubicin plus amlodipine.

by  $\text{Ca}^{2+}$  which is well-known to be able to increase the permeability of the mitochondrial membrane through the opened PT pore.<sup>24,33</sup> Dequalinium by blank mitosomes may also cause slight swelling of mitochondria, while liposomal daunorubicin plus amlodipine does not affect the mitochondrial configuration in a short time exposure (30 min) due to the absence of dequalinium. The above alterations in the mitochondria after applying mitosomes could therefore be evidence for the opening of the PT pore.

In the measurement of  $\Delta\Psi_m$ , a significant dissipation of  $\Delta\Psi_m$  for cancer cells after being exposed to mitosomes indicates that the loaded drugs in mitosomes are released into the mitochondria and induce the dissipation of  $\Delta\Psi_m$ . The  $\Delta\Psi_m$  value of complete mitochondria is very high due to the proton gradient requested for ATP production; however, when a PT pore opens, the permeability of the mitochondrial membrane increases, leading to an influx of solutes and ions, resulting in the equilibrium of protons, and thereby inducing the collapse of  $\Delta\Psi_m$ .<sup>34,35</sup> Accordingly, loss of  $\Delta\Psi_m$  is additional evidence of the opening of the PT pore.<sup>26</sup>

Results from immunohistochemical staining indicate that mitosomal daunorubicin plus amlodipine results in an eminent translocation of cytochrome C. Two mechanisms

(33) Yamamoto, T.; Tachikawa, A.; Terauchi, S.; Yamashita, K.; Kataoka, M.; Terada, H.; Shinohara, Y. Multiple effects of DiS-C3(5) on mitochondrial structure and function. *Eur. J. Biochem.* **2004**, *271*, 3573–9.

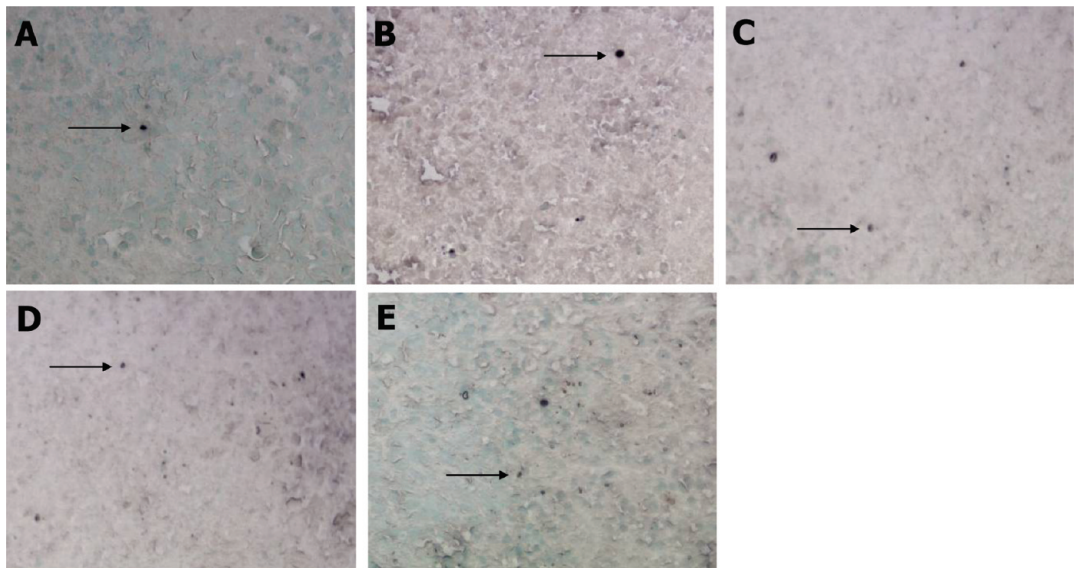


**Figure 9.** Paraffin sections showing TUNEL-labeled cells in the tumor tissues ( ×100) and apoptotic cells (shown by arrowhead) were characterized by a dense staining of nuclei. The MCF-7/adr xenografted mice were intravenously treated with (A) physiological saline, (B) free daunorubicin (7 mg/kg) plus free amlodipine (7.04 mg/kg, mole ratio 1:1), (C) liposomal daunorubicin (7 mg/kg), (D) liposomal daunorubicin (7 mg/kg) plus amlodipine (7.04 mg/kg, mole ratio 1:1), and (E) mitosomal daunorubicin (7 mg/kg) plus amlodipine (7.04 mg/kg, mole ratio 1:1), respectively.

**Table 1.** Effect on the Hematological Indicators of Bone Marrow, Liver Function and Renal Function Following Intravenously Administration of Mitosomal Daunorubicin plus Amlodipine to Normal Kunming Mice via Tail Vein at Day 3, 5, 8, 10, and 12<sup>a</sup>

indicators	blank control	free daunorubicin plus free amlodipine	liposomal daunorubicin	liposomal daunorubicin plus amlodipine	mitosomal daunorubicin plus amlodipine
Bone Marrow					
WBC (10 <sup>9</sup> /L)	3.50 ± 0.48	1.74 ± 0.49*	2.02 ± 0.57*	1.56 ± 0.22*	2.88 ± 0.25
Hb (g/L)	18.40 ± 4.22	13.60 ± 4.77	17.25 ± 5.25	14.67 ± 2.52	14.75 ± 6.13
PLT (10 <sup>9</sup> /L)	522.60 ± 176.33	217.20 ± 155.81*	336.75 ± 106.60	345.00 ± 44.14	343.40 ± 63.34
Liver Function					
ALT (IU/L)	41.50 ± 1.91	59.60 ± 4.72*	42.50 ± 4.20	45.60 ± 7.54	45.80 ± 6.50
AST (IU/L)	204.50 ± 25.62	306.25 ± 98.44	241.67 ± 21.01	229.25 ± 60.65	212.67 ± 13.87
TB μmol/L)	1.57 ± 0.31	1.94 ± 0.29	1.53 ± 0.10	1.75 ± 0.30	1.98 ± 0.43
Renal Function					
urea (mmol/L)	11.64 ± 1.16	11.98 ± 4.65	10.45 ± 1.55	13.13 ± 2.09	13.38 ± 1.30
Cre μmol/L)	34.80 ± 5.07	42.00 ± 5.79	41.25 ± 3.59	43.50 ± 4.20	42.20 ± 2.17

<sup>a</sup>\**P* < 0.05, versus blank control.

are involved in the process. The first is associated with the opening of the mitochondrial permeability transition (PT) pore<sup>36</sup> which induces the swelling of mitochondrial matrix, results in the rupture of the outer membrane,<sup>37</sup> and thereby causes the spillage of cytochrome C. The second mechanism is through channels formed by protein aggregates induced by Bax, which is a pro-apoptotic gene encoding protein belonging to Bcl-2 family,<sup>38,39</sup> as further explained in the following passage.

The Bid assay demonstrates that mitosomal daunorubicin plus amlodipine leads to an obvious cleavage of Bid, followed by activating Bax, which is then inserted into the outer mitochondria membrane, and aggregated to form channels through which cytochrome C is released to the cytosol, resulting in a cascade of apoptosis.<sup>39,40</sup> In these processes, Bax may be also coactivated by Bcl-2/Bcl-X<sub>L</sub> suppression<sup>37,41</sup> triggered by the mitochondria. The cleavage

(34) Zoratti, M.; Szabo, I. The mitochondrial permeability transition. *Biochim. Biophys. Acta* **1995**, *1241*, 139–76.  
(35) Zamzami, N.; Marchetti, P.; Castedo, M.; Zanin, C.; Vayssiere, J. L.; Petit, P. X.; Kroemer, G. Reduction in mitochondrial potential constitutes an early irreversible step of programmed lymphocyte death in vivo. *J. Exp. Med.* **1995**, *181*, 1661–72.

(36) Kumarswamy, R.; Seth, R. K.; Dwarakanath, B. S.; Chandna, S. Mitochondrial regulation of insect cell apoptosis: evidence for permeability transition pore-independent cytochrome-c release in the Lepidopteran Sf9 cells. *Int. J. Biochem. Cell Biol.* **2009**, *41*, 1430–40.  
(37) Galluzzi, L.; Blomgren, K.; Kroemer, G. Mitochondrial membrane permeabilization in neuronal injury. *Nat. Rev. Neurosci.* **2009**, *10*, 481–94.

of Bid is the consequence of the activated caspase 8,<sup>42</sup> which is proved by the caspase 8 activity assays. In addition, there is another pathway in which the drugs released from the ruptured mitosomes induce the activation of caspase 8, which directly results in the activation of caspase 3, leading to a cascade of apoptosis, as evidenced by the caspase 3 activity assay. Actually, the activated caspase 3 could be derived from the activations of both the activated caspase 8 in the death receptor pathway in the cytosol and the activated caspase 9 in the mitochondrial pathway.

The results from the treatments with free drugs or their combinations in the antiproliferative activity assay demonstrate that amlodipine could enhance the anticancer efficacy of daunorubicin in both cells, indicating that amlodipine is not only an effective enhancer for increasing the anticancer efficacy in the nonresistant cancer cells but also a robust MDR reversing agent in the resistant cancer cells. Furthermore, the results demonstrate that the mitosomes are able to significantly reverse the MDR, thereby enhancing the anticancer effect in resistant cancer cells. However, the in vitro cytotoxicity of drug-loaded mitosomes is lower than that of free daunorubicin, or daunorubicin plus amlodipine. The possible reasons are that free drugs are directly exposed to cells so that they could be easily ingested by cancer cells, while the drug-loaded mitosomes or liposomes may retard the uptake rate due to membrane fusion between a liposome/mitosome and a tumor cell or endocytosis of a liposome/mitosome by a tumor cell.<sup>43</sup>

- (38) Jurgensmeier, J. M.; Xie, Z.; Deveraux, Q.; Ellerby, L.; Bredesen, D.; Reed, J. C. Bax directly induces release of cytochrome c from isolated mitochondria. *Proc. Natl. Acad. Sci. U.S.A.* **1998**, *95*, 4997–5002.
- (39) Shimizu, S.; Narita, M.; Tsujimoto, Y. Bcl-2 family proteins regulate the release of apoptogenic cytochrome c by the mitochondrial channel VDAC. *Nature* **1999**, *399*, 483–7.
- (40) Grohm, J.; Plesnila, N.; Culmsee, C. Bid mediates fission, membrane permeabilization and peri-nuclear accumulation of mitochondria as a prerequisite for oxidative neuronal cell death. *Brain Behav. Immun.* **2010**, *24*, 831–8. Epub 2009 Dec 2.
- (41) Dlugosz, P. J.; Billen, L. P.; Annis, M. G.; Zhu, W.; Zhang, Z.; Lin, J.; Leber, B.; Andrews, D. W. Bcl-2 changes conformation to inhibit Bax oligomerization. *EMBO J.* **2006**, *25*, 2287–96.
- (42) Tsujimoto, Y. Role of Bcl-2 family proteins in apoptosis: apoptosomes or mitochondria? *Genes Cells* **1998**, *3*, 697–707.
- (43) Wrobel, I.; Collins, D. Fusion of cationic liposomes with mammalian cells occurs after endocytosis. *Biochim. Biophys. Acta* **1995**, *1235*, 296–304.

The inhibitory effects in the resistant MCF-7/adr cells xenografted nude mice demonstrate that the mitosomes are able to effectively enhance the anticancer activity of the resistant cancers in vivo, and the TUNEL analysis demonstrates that mitosomal daunorubicin plus amlodipine provides the most significantly inducing apoptotic effects, and the result is consistent with that observed from the inhibition of tumor growth. As compared to the data in vitro, the drug-loaded mitosomes are more effective than free drugs in vivo. This could be explained by the facts that the PEGylated mitosomes are able to avoid the rapid uptake by the reticuloendothelial system (RES), and could accumulate more in the tumor tissues by the enhanced permeability and retention effect (EPR effect). In contrast, two free drugs may be less simultaneously distributed in the tumor site because of the differences in pharmacokinetic property for each drug.

After administering mitosomal daunorubicin plus amlodipine by multiple intravenous injections to normal mice, liver function indicators (ALT, AST, and TB) and kidney function indicators (urea and Cre) are slightly elevated, while bone marrow indicators (WBC, Hb, and PLT) are mildly lowered, suggesting that mitosomal daunorubicin plus amlodipine may have no significant influences on the liver, kidney or bone marrow. At least, the potential toxic effects may be no more than those after administering free daunorubicin plus amlodipine.

In conclusion, we proposed here a type of cancer mitochondria-specifically targeting nanovesicles, daunorubicin plus amlodipine mitosomes, toward a complete solution to the intrinsic multidrug resistance of cancers. The drug-loaded mitosomes could selectively be accumulated in mitochondria, induce swelling and disruption of mitochondria, dissipate the mitochondrial potential, and result in a release of cytochrome C, cleavage of Bid, and activation of caspase 8 and 3. The enhanced anticancer efficacy is evidenced in breast cancer MCF-7 and MCF-7/adr cells in vitro and MCF-7/adr xenografts in nude mice.

**Acknowledgment.** This study was supported by the Key Grant of Beijing Natural Science Foundation (No. 7091005), in part by the National Natural Science Foundation of China (No. 30772664), and the National Key Science Research Program of China (973 program, 2009CB930300). MP100249X